Tracer diffusion coefficients in a sheared inelastic Maxwell gas

Vicente Garzó[1,3], and Emmanuel Trizac[2,4]

[1] Departamento de Física and Instituto de Computación Científica Avanzada (ICCAEx), Universidad de Extremadura, E-06071 Badajoz, Spain

[2] Laboratoire de Physique Théorique et Modèles Statistiques (CNRS UMR 8626), Bâtiment 100, Université Paris-Sud, 91405 Orsay cedex, France

E-mail: vicenteg@unex.es and trizac@lptms.u-psud.fr

J. Stat. Mech. (2016) 073206

Abstract. We study the transport properties of an impurity in a sheared granular gas, in the framework of the Boltzmann equation for inelastic Maxwell models. We investigate here the impact of a nonequilibrium phase transition found in such systems, where the tracer species carries a finite fraction of the total kinetic energy (ordered phase). To this end, the diffusion coefficients are first obtained for a granular binary mixture in spatially inhomogeneous states close to the simple shear flow. In this situation, the set of coupled Boltzmann equations are solved by means of a Chapman–Enskog-like expansion around the (local) shear flow distributions for each species, thereby retaining all the hydrodynamic orders in the shear rate a. Due to the anisotropy induced by the shear flow, three tensorial quantities D_{ij}, $D_{p,ij}$, and $D_{T,ij}$ are required to describe the mass transport process instead of the conventional scalar coefficients. These tensors are given in terms of the solutions of a set of coupled algebraic equations, which can be *exactly* solved as functions of the shear rate a, the coefficients of restitution α_{sr} and the parameters of the mixture (masses and composition). Once the forms of D_{ij}, $D_{p,ij}$, and $D_{T,ij}$ are obtained for arbitrary mole fraction $x_1 = n_1/(n_1 + n_2)$ (where n_r is the number density of species r), the tracer limit $(x_1 \to 0)$ is carefully considered for the above three diffusion tensors. Explicit forms for these coefficients are derived showing that their shear rate dependence is significantly affected by the order-disorder transition.

[3] www.unex.es/eweb/fisteor/vicente/
[4] www.lptms.u-psud.fr/membres/trizac/

Contents

1. Introduction

The model of smooth inelastic hard spheres (IHS) has proven insightful to characterize the influence of collisional dissipation on the dynamic properties of rapid granular flows [1, 2]. Following this minimal route, the inelasticity of collisions is accounted for by a constant (positive) coefficient of normal restitution $\alpha \leqslant 1$ that only impinges on the translational degrees of freedom of grains [1]. The case $\alpha = 1$ stems for elastic, kinetic energy conserving collisions. On the other hand, the complex mathematical structure of the Boltzmann collision operator for IHS prevents us from obtaining exact results, even in the simplest homogeneous cooling state. To get the explicit forms of

the Navier–Stokes transport coefficients [3] one usually considers the leading order in a Sonine polynomial expansion of the velocity distribution function [1, 2]. These difficulties increase considerably when one studies multicomponent systems (namely, a mixture of grains with different masses, sizes and coefficients of restitution) since not only the number of transport coefficients is larger than for a single gas but also the kinetic description involves a set of coupled Boltzmann equations for the one-particle velocity distribution function of each species.

One of the main mathematical intricacies in evaluating the collisional moments of the Boltzmann operator for hard spheres (even for ordinary mixtures) comes from the fact that the collision rate is proportional to the magnitude of the relative velocity of the two colliding spheres. This property precludes the possibility of determining those collisional moments without the knowledge of the velocity distribution functions. In the case of elastic fluids, a possible way to overcome this problem (keeping the structure of the Boltzmann collision operator) is to assume that the particles interact via the repulsive Maxwell potential (inversely proportional to the fourth power of the distance). For this interaction model, the collision rate is independent of the relative velocity and this brings a number of convenient mathematical properties of the Boltzmann collision operator [4]. Thanks to this simplification, nonlinear transport properties can be exactly obtained [5, 6] from the Boltzmann equation for Maxwell elastic molecules and, when properly reduced, they exhibit a good agreement with results obtained for other interaction models [7]. In the context of inelastic gases, the Boltzmann equation for inelastic Maxwell models (IMM) was also introduced about sixteen years ago [8]. The IMM share with elastic Maxwell molecules the property that the collision rate is velocity *independent* but their collision rules are the same as for IHS. Although these IMM's do not describe real particles since they do not interact according to a given potential law, it must be stressed that several results derived from IMM [9–13] agree well with the predictions made from IHS. Moreover, in the framework of the Boltzmann equation, Maxwell models can be introduced at the level of the cross section without any reference to a specific interaction potential [4, 14]. It is here noteworthy that some experiments [15] for magnetic grains with dipolar interactions are well described by IMM.

One of the most widely studied states in granular gases is the so-called simple or uniform shear flow (USF) state. In the case of a binary granular mixture, it is characterized by constant partial densities n_r ($r = 1, 2$), a uniform granular temperature T, and a linear velocity profile $u_x = u_{1x} = u_{2x} = ay$ where a is the constant shear rate and $\mathbf{u}_r$ denotes the mean velocity of species r. In this problem, the mass and heat fluxes vanish by symmetry and hence, the pressure tensor P is the relevant flux of the problem. In the case of IMM, the elements of the pressure tensor were exactly determined [16] in terms of the shear rate and the parameters of the mixture. Subsequently, the dynamics of an impurity immersed in an inelastic Maxwell gas under USF was studied [17, 18] by starting from the above exact solution [16] (which holds for arbitrary concentration $x_r = n_r/(n_1 + n_2)$) and taking carefully the tracer limit (i.e. when the concentration of one of the species becomes negligible). Surprisingly, a non-equilibrium phase transition was identified with a region ('ordered' phase) where the contribution of impurities to the total kinetic energy is *finite*. This unexpected behaviour was present when the gas is sheared or when it evolves freely (namely, in the so-called homogeneous

cooling state) [19]. In this latter case, we have recently analyzed [20] the impact of this transition on the Navier–Stokes transport coefficients, showing that those coefficients exhibit a different dependence on the mass ratios and the coefficients of restitution in the 'ordered' and 'disordered' phases.

The aim of this paper is to gauge the effect of the above non-equilibrium transition on the transport properties associated with impurities when the granular gas is shear flow driven. As in the previous study [20] for the Navier–Stokes coefficients, in order to determine in a clean way the behaviour of the tracer transport coefficients in both non-equilibrium phases, one has first to evaluate transport around USF for a general binary mixture (i.e. with $x_1 \neq 0$) and then take the corresponding tracer limit ($x_1 \to 0$). This first requires the computation of the complete set of generalized transport coefficients of a granular binary mixture (with $x_1 \neq 0$) in a state that deviates from the USF by small spatial gradients. To get those coefficients, one should solve the set of coupled Boltzmann equations by means of a Chapman–Enskog-like method around the (local) shear flow distributions for each species that retain all the hydrodynamic orders in the shear rate. This is the essential difference with respect to the conventional Chapman–Enskog method [21]. Since the base state (zeroth-order approximation) is anisotropic, tensorial quantities are required to describe the irreversible fluxes instead of scalar coefficients. The evaluation of these generalized tensors has been recently carried out by the authors of the present paper [22]. On the other hand, due to the technical difficulties involved in explicitly computing the shear-rate dependence of the transport coefficients, only the mass transport of impurities was evaluated. This flux is characterized by the second-rank tensors D_{ij} (diffusion tensor), $D_{p,ij}$ (pressure diffusion tensor) and $D_{T,ij}$ (thermal diffusion tensor). Here, we will explicitly compute the above shear-rate dependent diffusion coefficients in the tracer limit. The results show that the dependence of those coefficients on the shear rate and the parameters of the mixture is clearly different in both ordered and disordered phases.

The plan of the paper is as follows. In section 2 we introduce the Boltzmann equation for IMM and present the USF problem. In addition, the tracer limit is also considered and the ordered phases where impurities bear a finite contribution to the properties of the mixture are identified. Section 3 deals with the description of the Chapman–Enskog-like method to get the diffusion coefficients D_{ij}, $D_{p,ij}$ and $D_{T,ij}$. The algebraic equations defining those coefficients are explicitly written in section 4 for arbitrary concentration. Then, starting from the above general expressions, we derive their forms in the ordered and disordered phases when the tracer limit is considered. The dependence of the above coefficients on the parameter space of the problem is illustrated in section 5 for systems where impurities are lighter or heavier than the particles of the granular gas. Finally, we conclude in section 6 with a brief discussion of the main findings of the paper.

2. Inelastic Maxwell mixtures under shear flow

2.1. Boltzmann kinetic equation

Let us consider a granular binary mixture modeled as an inelastic Maxwell model. In the simplest version, the Boltzmann equation for IMM [8] can be obtained from

the Boltzmann equation for IHS by replacing the rate for collisions between particles of species r and s by an average velocity-independent collision rate. With this simplification and in the absence of external forces, the set of nonlinear Boltzmann kinetic equations becomes

$$\left(\frac{\partial}{\partial t} + \mathbf{v} \cdot \nabla\right) f_r(\mathbf{r}, \mathbf{v}; t) = \sum_{s=1}^{2} J_{rs}[\mathbf{v}| f_r(t), f_s(t)], \tag{1}$$

where $f_r(\mathbf{r}, \mathbf{v}, t)$ is the one-particle distribution function of species r ($r = 1, 2$) and the Boltzmann collision operator $J_{rs}[\mathbf{v}_1| f_r, f_s]$ for IMM describing the scattering of pairs of particles is

$$J_{rs}[\mathbf{v}_1| f_r, f_s] = \frac{\omega_{rs}}{n_s \Omega_d} \int \mathrm{d}\mathbf{v}_2 \int \mathrm{d}\widehat{\boldsymbol{\sigma}}[\alpha_{rs}^{-1} f_r(\mathbf{r}, \mathbf{v}_1', t) f_s(\mathbf{r}, \mathbf{v}_2', t) - f_r(\mathbf{r}, \mathbf{v}_1, t) f_s(\mathbf{r}, \mathbf{v}_2, t)]. \tag{2}$$

In equation (2),

$$n_r = \int \mathrm{d}\mathbf{v} f_r(\mathbf{v}) \tag{3}$$

is the number density of species r, ω_{rs} is an effective collision frequency for collisions of type r-s, $\Omega_d = 2\pi^{d/2}/\Gamma(d/2)$ is the total solid angle in d dimensions, and $\alpha_{rs} \leqslant 1$ refers to the constant coefficient of restitution for collisions between particles of species r with s. In addition, the primes on the velocities denote the initial values $\{\mathbf{v}_1', \mathbf{v}_2'\}$ that lead to $\{\mathbf{v}_1, \mathbf{v}_2\}$ following a binary collision:

$$\mathbf{v}_1' = \mathbf{v}_1 - \mu_{sr}(1 + \alpha_{rs}^{-1})(\widehat{\boldsymbol{\sigma}} \cdot \mathbf{g}_{12})\widehat{\boldsymbol{\sigma}}, \tag{4}$$

$$\mathbf{v}_2' = \mathbf{v}_2 + \mu_{rs}(1 + \alpha_{rs}^{-1})(\widehat{\boldsymbol{\sigma}} \cdot \mathbf{g}_{12})\widehat{\boldsymbol{\sigma}}, \tag{5}$$

where $\mathbf{g}_{12} = \mathbf{v}_1 - \mathbf{v}_2$ is the relative velocity of the colliding pair, $\widehat{\boldsymbol{\sigma}}$ is a unit vector directed along the centers of the two colliding spheres, and $\mu_{rs} = m_r/(m_r + m_s)$.

The effective collision frequencies ω_{rs} are independent of velocity but depend in general on space an time through their dependence on density and temperature. As in previous works [17–19], we will consider a simple version of IMM ('plain vanilla Maxwell model') where one defines ω_{rs} as

$$\omega_{rs} = x_s \nu_0, \quad \nu_0 = An, \tag{6}$$

where $x_s = n_s/n$ is the concentration or mole fraction of species s and the value of the constant A is irrelevant for our purposes. Here, $n = n_1 + n_2$ is the total number density of the mixture. The form of ω_{rs} is closer to the original model of Maxwell molecules for elastic mixtures [6]. This plain vanilla model has been previously employed by several authors [23, 24] and it is capable of capturing the essential physical effects in shearing problems [10, 18].

At a hydrodynamic level, apart from the partial densities n_r, the relevant quantities in a binary mixture are the flow velocity $\mathbf{u}$, and the 'granular' temperature T. They are defined as

$$\rho \mathbf{u} = \sum_r \rho_r \mathbf{u}_r = \sum_r \int \mathrm{d}\mathbf{v} m_r \mathbf{v} f_r(\mathbf{v}), \tag{7}$$

$$nT = \sum_r n_r T_r = \sum_r \int \mathrm{d}\mathbf{v} \frac{m_r}{d} V^2 f_r(\mathbf{v}), \tag{8}$$

where $\rho_r = m_r n_r$, $\rho = \rho_1 + \rho_2$ is the total mass density, and $\mathbf{V} = \mathbf{v} - \mathbf{u}$ is the peculiar velocity. Apart from the hydrodynamic fields, an interesting quantity is the partial temperature T_r of species r defined as

$$n_r T_r = \int \mathrm{d}\mathbf{v} \frac{m_r}{d} V^2 f_r(\mathbf{v}). \tag{9}$$

The partial temperature T_r measures the mean kinetic energy of species r. As confirmed by computer simulations [25], experiments [26, 27] and kinetic theory calculations [28, 29], the global granular temperature T is in general different from the partial temperatures T_r. In addition, the mass flux $\mathbf{j}_r$ of species r, the pressure tensor P and the heat flux $\mathbf{q}$ are given, respectively, by

$$\mathbf{j}_r = m_r \int \mathrm{d}\mathbf{v}\, \mathbf{V} f_r(\mathbf{v}), \tag{10}$$

$$\mathsf{P} = \sum_r \int \mathrm{d}\mathbf{v}\, m_r \mathbf{V}\mathbf{V} f_r(\mathbf{v}), \tag{11}$$

$$\mathbf{q} = \sum_r \int \mathrm{d}\mathbf{v}\, \frac{1}{2} m_r V^2 \mathbf{V} f_r(\mathbf{v}). \tag{12}$$

Finally, the rate of energy dissipated due to collisions among all species defines the (total) cooling rate ζ as

$$\sum_r \sum_s m_r \int \mathrm{d}\mathbf{v}\, V^2 J_{rs}[\mathbf{v}|\, f_r, f_s] = -dnT\zeta. \tag{13}$$

Equation (11) also defines the partial contribution P_r of species r to the total pressure tensor P as

$$\mathsf{P}_r = \int \mathrm{d}\mathbf{v}\, m_r \mathbf{V}\mathbf{V} f_r(\mathbf{v}). \tag{14}$$

Note that $\mathbf{j}_1 = -\mathbf{j}_2$ due to the definition (10).

2.2. Uniform shear flow

Let us assume that the mixture is under USF. This state is macroscopically characterized by constant densities, a uniform temperature, and a linear velocity profile

$$\mathbf{u}(y) = \mathbf{u}_1(y) = \mathbf{u}_2(y) = ay\widehat{\mathbf{x}}, \tag{15}$$

where a is the constant shear rate. This profile assumes no boundary layer near the walls and is generated by the Lees–Edwards boundary conditions [30], which are simply periodic boundary conditions in the local Lagrange frame moving with the flow velocity [31]. Thus, at a microscopic level, the velocity distribution functions f_s of the USF state become *uniform* when one refers the velocity of the particles to the local Lagrangian

frame moving at the flow velocity defined by equation (15), i.e. $f_s(\mathbf{r}, \mathbf{v}, t) = f_s(\mathbf{V}, t)$. In that case, equation (1) can be written as [6]

$$\frac{\partial}{\partial t} f_1 - a V_y \frac{\partial}{\partial V_x} f_1 = J_{11}[f_1, f_1] + J_{12}[f_1, f_2]. \tag{16}$$

A similar equation holds for f_2.

Since n_s and T are uniform in the USF state, then the mass and heat fluxes vanish and the pressure tensor is the only non-vanishing flux of the problem. Moreover, the only relevant balance equation is that for the temperature. It can be obtained from equation (16) and its counterpart for species 2; it is given by

$$\nu_0^{-1} \frac{\partial}{\partial t} \ln T = -\zeta^* - \frac{2a^*}{d} P_{xy}^*, \tag{17}$$

where $\zeta^* \equiv \zeta/\nu_0$, $a^* \equiv a/\nu_0$, and $P_{xy}^* \equiv P_{xy}/p$. Here, $p = nT$ is the hydrostatic pressure. In the USF problem, the expression for ζ^* is [10]

$$\zeta^* = \frac{2}{d} \sum_r \sum_s x_r x_s \mu_{sr}(1 + \alpha_{rs})\left[\gamma_r - \frac{1 + \alpha_{rs}}{2}(\gamma_r \mu_{sr} + \gamma_s \mu_{rs})\right], \tag{18}$$

where $\gamma_r \equiv T_r/T$ and use has been made of the property $\mathbf{j}_r = \mathbf{0}$. The *reduced* shear rate a^* is the nonequilibrium relevant parameter of the USF problem since it measures the distance of the system from the homogeneous cooling state ($a^* = 0$). According to equation (17), the temperature changes in time due to the competition of two opposite mechanisms: on the one hand, viscous heating ($-a^* P_{xy}^* > 0$) and, on the other hand, energy dissipation in collisions ($-\zeta^* < 0$). In general, since a^* does not depend on time, there is no steady state unless a^* takes the specific value given by the steady-state condition

$$a_s^* P_{s,xy}^* = -\frac{d}{2} \zeta_s^*, \tag{19}$$

where a_s^*, $P_{s,xy}^*$ and ζ_s^* denotes the steady-state values of the (reduced) shear rate, the pressure tensor and the cooling rate, respectively. Beyond this particular case, the (reduced) shear rate and the coefficients of restitution are not coupled and hence, one can study the combined effect on both quantities on the elements of the pressure tensor of the mixture.

The explicit forms of the (scaled) pressure tensors $P_{r,ij}^* = P_{r,ij}/p$ have been obtained in [16] as nonlinear functions of the (reduced) shear rate, the coefficients of restitution and the parameters of the mixture (masses and concentration). Their expressions are displayed in appendix A. In particular, for long times, the temperature behaves as

$$T(t) = T(0) e^{\lambda \nu_0 t}, \tag{20}$$

where λ is the largest root of a sixth-degree polynomial equation with coefficients depending on a^*, α_{rs}, x_1 and the mass ratio $\mu \equiv m_1/m_2$. The results obtained in [18] for $x_1 \neq 0$ show that, at a given value of a^*, the difference between the two largest roots of the above sixth-degree equation does not vanish. This means that the asymptotic time dependence of the partial pressure tensors $P_{r,ij}^*$ is always ruled by one of the roots.

2.3. Tracer limit ($x_1 \to 0$)

We assume now that the concentration of one of the species (say for instance, species 1) becomes negligible. In the tracer limit ($x_1 \to 0$), the sixth-degree equation for λ factorizes into two cubic equations with the following largest roots:

$$\lambda_2^{(0)} = \frac{(1+\alpha_{22})^2}{d+2}F(\tilde{a}) - \frac{1-\alpha_{22}^2}{2d}, \tag{21}$$

$$\lambda_1^{(0)} = \frac{2\mu_{21}^2}{d+2}(1+\alpha_{12})^2 F\left(\frac{\tilde{a}}{2\mu_{21}^2}\frac{(1+\alpha_{22})^2}{(1+\alpha_{12})^2}\right) - \frac{2}{d}\mu_{21}(1+\alpha_{12})\left[1 - \frac{\mu_{21}}{2}(1+\alpha_{12})\right], \tag{22}$$

where

$$F(x) \equiv \frac{2}{3}\sinh^2\left[\frac{1}{6}\cosh^{-1}\left(1 + \frac{27}{d}x^2\right)\right] \tag{23}$$

and

$$\tilde{a} = \frac{2(d+2)}{(1+\alpha_{22})^2}a^*. \tag{24}$$

The root $\lambda_2^{(0)}$ rules the dynamics of the host fluid (excess component) while the evolution of the tracer species is governed by $\lambda_1^{(0)}$.

As said before, the largest of all roots, $\lambda_{\max}$, is the relevant one to obtain the asymptotic values of the (scaled) pressure tensors P_r^*. In particular, the energy ratio $E_1/E = x_1\gamma_1$ (or equivalently, the reduced partial pressure $p_1^* = n_1 T_1/p$) can be easily obtained from the pressure tensor P_1^* associated with the tracer particles. It was shown in [17, 18] that the behaviour of the system is qualitatively very different depending on $\lambda_{\max} = \lambda_1^{(0)}$ or $\lambda_{\max} = \lambda_2^{(0)}$. Thus, when $\lambda_2^{(0)} > \lambda_1^{(0)}$, $E_1/E = 0$ when $x_1 \to 0$ as expected and $T_1/T_2 \equiv$ finite. This region of the parameter space is coined as the 'disordered' phase.

On the other hand, if $\lambda_1^{(0)} > \lambda_2^{(0)}$, then $T_1/T_2 \to \infty$ but surprisingly $E_1/E \neq 0$. We found two different families of 'ordered' phase:

- A light impurity phase which is present when $a^* > a_c^*(\mu, \alpha_{rs})$ and $\mu < \mu_{\text{th}}^{(-)}$ where

$$\mu_{\text{th}}^{(-)} = \sqrt{2}\frac{1+\alpha_{12}}{1+\alpha_{22}} - 1. \tag{25}$$

  This phase can also be observed at vanishing shear rate ($a^* = 0$) when the mass ratio $\mu > \mu_{\text{HCS}}^{(+)}$ or $\mu < \mu_{\text{HCS}}^{(-)}$ where [19]

$$\mu_{\text{HCS}}^{(-)} = \frac{\alpha_{12} - \sqrt{\frac{1+\alpha_{22}^2}{2}}}{1 + \sqrt{\frac{1+\alpha_{22}^2}{2}}}, \quad \mu_{\text{HCS}}^{(+)} = \frac{\alpha_{12} + \sqrt{\frac{1+\alpha_{22}^2}{2}}}{1 - \sqrt{\frac{1+\alpha_{22}^2}{2}}}. \tag{26}$$

Note that while the upper bound $\mu_{\mathrm{HCS}}^{(+)}$ is well defined for all values of α_{12} and α_{22}, the lower one is only positive when $\alpha_{12} > \sqrt{(1+\alpha_{22})^2/2}$ (asymmetric dissipation).

- A heavy impurity phase ($\mu > \mu_{\mathrm{HCS}}^{(+)}$), which cannot accommodate large shear rates and requires $a^* < a^{*(+)}$, where

$$a^{*(+)} = \frac{1 + d - \alpha_{22}}{d} \sqrt{\frac{1-\alpha_{22}^2}{2(d+2)}}. \tag{27}$$

The existence of the light impurity ordered phase was already found years ago for elastic collisions [32]. The explicit form of E_1/E is provided[5] in the appendix C of [18]. Note that the above results do not depend of the impurity-impurity coefficient of restitution α_{11}, which is intuitively expected.

As alluded to in the Introduction, the goal here is to analyze the fingerprint of this nonequilibrium transition on the diffusion coefficients associated to the tracer species. In order to do it, we have to determine them first for *arbitrary* x_1. This will be carried out in the next section by solving the Boltzmann equation of the mixture by means of a Chapman–Enskog-like expansion.

3. Chapman–Enskog-like expansion around USF

We assume now that we excite the USF by small spatial perturbations, in order to get the diffusion transport coefficients associated with the mass flux. We start from the set of Boltzmann equations (1) with a general time and space dependence. Let $u_{0,i} = a_{ij}r_j$ be the flow velocity of the *undisturbed* USF state, where $a_{ij} = a\delta_{ix}\delta_{jy}$. In the *disturbed* state however, the true velocity $\mathbf{u}$ is in general different from $\mathbf{u}_0$ [33–35], i.e. $u_i = u_{0,i} + \delta u_i$, δu_i being a small perturbation to $u_{0,i}$. Thus, in the perturbed USF state, the peculiar velocity is $\mathbf{c} = \mathbf{V} - \delta\mathbf{u}$, where $\mathbf{V} = \mathbf{v} - \mathbf{u}_0$. In the Lagrangian frame moving with $\mathbf{u}_0$, the Boltzmann equations (1) reads

$$\frac{\partial}{\partial t}f_1 - aV_y\frac{\partial}{\partial V_x}f_1 + (\mathbf{V}+\mathbf{u}_0)\cdot\nabla f_1 = J_{11}[f_1,f_1] + J_{12}[f_1,f_2], \tag{28a}$$

$$\frac{\partial}{\partial t}f_2 - aV_y\frac{\partial}{\partial V_x}f_2 + (\mathbf{V}+\mathbf{u}_0)\cdot\nabla f_2 = J_{22}[f_2,f_2] + J_{21}[f_2,f_1], \tag{28b}$$

where the derivative ∇f_r is taken at constant $\mathbf{V}$. The macroscopic balance equations follow as

$$\partial_t n_r + \mathbf{u}_0\cdot\nabla n_r + \nabla\cdot(n_r\delta\mathbf{u}) = -\frac{\nabla\cdot\mathbf{j}_r}{m_r}, \quad (r=1,2), \tag{29}$$

---

[5] While we were working on this paper, we have realized that there were some typos in the expressions given in [18] for the coefficients $A_{11}^{(1)}$, $A_{22}^{(1)}$ and $B_{22}^{(1)}$. The forms displayed here for these quantities correct the above typos. On the other hand, the final expression of the energy ratio E_1/E provided in [18] is correct.

$$\partial_t \delta u_i + a_{ij}\delta u_j + (\mathbf{u}_0 + \delta\mathbf{u}) \cdot \nabla \delta u_i = -\rho^{-1}\nabla_j P_{ij}, \tag{30}$$

$$\frac{d}{2}n\partial_t T + \frac{d}{2}n(\mathbf{u}_0 + \delta\mathbf{u}) \cdot \nabla T = -aP_{xy} - \frac{d}{2}T\sum_r \frac{\nabla \cdot \mathbf{j}_r}{m_r} - \left(\nabla \cdot \mathbf{q} + \mathsf{P} : \nabla \delta\mathbf{u} + \frac{d}{2}p\zeta\right), \tag{31}$$

where the mass flux $\mathbf{j}_r$, the pressure tensor P, the heat flux $\mathbf{q}$, and the cooling rate ζ are defined by equations (10)–(13), respectively, with the replacement $\mathbf{V} \to \mathbf{c}$.

The deviations from the USF state are assumed small; the spatial gradients of the hydrodynamic fields are thus small as well. Here, as in previous works on granular mixtures [36], we chose the mole fraction x_1, the pressure p, the temperature T, and the local flow velocity $\delta\mathbf{u}$ as the relevant hydrodynamic fields. Since the system is strongly sheared, a solution to the set of Boltzmann equations (28a) and (28b) can be obtained by means of a generalization of the conventional Chapman–Enskog method [21] in which the velocity distribution function is expanded around a *local* shear flow reference state in terms of the small spatial gradients of the hydrodynamic fields relative to those of USF. This is the main new ingredient of the expansion.

This type of Chapman–Enskog-like expansion has been already considered to get the set of shear-rate dependent transport coefficients for monodisperse systems in the case of inelastic hard spheres [33, 34] and inelastic Maxwell models [35]. More recently, the method has been extended to the case of granular mixtures [22]. Since the procedure involved in the evaluation of the first-order approximation to the mass flux (which is the quantity needed to analyze the diffusion coefficients) has been widely exposed in [22], we will start here our study on tracer diffusion coefficients by adapting the results derived in this paper [22] to the special vanilla Maxwell model (see equation (6)). More technical details on the application of the Chapman–Enskog-like method can be found in the latter reference.

3.1. First-order approximation to the mass flux

To first order in the gradients, the mass flux $\mathbf{j}_1^{(1)}$ of species 1 is given by

$$j_{1,i}^{(1)} = -\frac{m_1 m_2 n}{\rho}D_{ij}\frac{\partial x_1}{\partial r_j} - \frac{\rho}{p}D_{p,ij}\frac{\partial p}{\partial r_j} - \frac{\rho}{T}D_{T,ij}\frac{\partial T}{\partial r_j}, \quad j_{2,i}^{(1)} = -j_{1,i}^{(1)}. \tag{32}$$

The diffusion tensors D_{ij}, $D_{p,ij}$, and $D_{T,ij}$ are defined as

$$D_{ij} = -\frac{\rho}{nm_2}\int d\mathbf{c}\, c_i\, \mathcal{A}_{1,j}(\mathbf{c}), \tag{33}$$

$$D_{p,ij} = -\frac{pm_1}{\rho}\int d\mathbf{c}\, c_i\, \mathcal{B}_{1,j}(\mathbf{c}), \tag{34}$$

$$D_{T,ij} = -\frac{Tm_1}{\rho}\int d\mathbf{c}\, c_i\, \mathcal{C}_{1,j}(\mathbf{c}), \tag{35}$$

where $\boldsymbol{\mathcal{A}}_1(\mathbf{c})$, $\boldsymbol{\mathcal{B}}_1(\mathbf{c})$ and $\boldsymbol{\mathcal{C}}_1(\mathbf{c})$ are the solutions of the following set of linear integral equations:

$$\lambda \nu_0 (p\partial_p + T\partial_T)\boldsymbol{\mathcal{A}}_1 - ac_y \frac{\partial}{\partial c_x}\boldsymbol{\mathcal{A}}_1 + \mathcal{L}_1 \boldsymbol{\mathcal{A}}_1 + \mathcal{M}_1 \boldsymbol{\mathcal{A}}_2 = \mathbf{A}_1$$
$$+ \left(\frac{2a}{d}\frac{\partial P_{xy}^{(0)}}{\partial x_1} + p\frac{\partial \zeta^{(0)}}{\partial x_1} \right)\boldsymbol{\mathcal{B}}_1 + \left(\frac{2aT}{dp}\frac{\partial P_{xy}^{(0)}}{\partial x_1} + T\frac{\partial \zeta^{(0)}}{\partial x_1} \right)\boldsymbol{\mathcal{C}}_1, \tag{36}$$

$$\lambda \nu_0 (p\partial_p + T\partial_T)\boldsymbol{\mathcal{B}}_1 - \left[\frac{2a}{d}\partial_p P_{xy}^{(0)} + (1 + p\partial_p)\zeta^{(0)} + ac_y \frac{\partial}{\partial c_x} \right]\boldsymbol{\mathcal{B}}_1 + \mathcal{L}_1 \boldsymbol{\mathcal{B}}_1 + \mathcal{M}_1 \boldsymbol{\mathcal{B}}_2 = \mathbf{B}_1$$
$$- \left[\frac{2aT}{dp^2}(1 - p\partial_p)P_{xy}^{(0)} - \frac{T}{p}\partial_p \zeta^{(0)} \right]\boldsymbol{\mathcal{C}}_1, \tag{37}$$

$$\lambda \nu_0 (p\partial_p + T\partial_T)\boldsymbol{\mathcal{C}}_1 - \left[(1 + T\partial_T)\left(\frac{2a}{dp}P_{xy}^{(0)} + \zeta^{(0)} \right) + ac_y \frac{\partial}{\partial c_x} \right]\boldsymbol{\mathcal{C}}_1 + \mathcal{L}_1 \boldsymbol{\mathcal{C}}_1 + \mathcal{M}_1 \boldsymbol{\mathcal{C}}_2 = \mathbf{C}_1$$
$$+ \left[\partial_T \left(\frac{2a}{d}P_{xy}^{(0)} + p\zeta^{(0)} \right) \right]\boldsymbol{\mathcal{B}}_1. \tag{38}$$

Here, we have introduced the quantities

$$A_{1,i}(\mathbf{c}) = -\frac{\partial f_1^{(0)}}{\partial x_1}c_i - \frac{1}{\rho}\frac{\partial f_1^{(0)}}{\partial c_j}\frac{\partial P_{ij}^{(0)}}{\partial x_1}, \tag{39}$$

$$B_{1,i}(\mathbf{c}) = -\frac{\partial f_1^{(0)}}{\partial p}c_i - \frac{1}{\rho}\frac{\partial f_1^{(0)}}{\partial c_j}\frac{\partial P_{ij}^{(0)}}{\partial p}, \tag{40}$$

$$C_{1,i}(\mathbf{c}) = -\frac{\partial f_1^{(0)}}{\partial T}c_i - \frac{1}{\rho}\frac{\partial f_1^{(0)}}{\partial c_j}\frac{\partial P_{ij}^{(0)}}{\partial T}. \tag{41}$$

Moreover, $\mathcal{L}_1$ and $\mathcal{M}_1$ are the linearized Boltzmann collision operators around the reference USF state:

$$\mathcal{L}_1 X = -(J_{11}[f_1^{(0)}, X] + J_{11}[X, f_1^{(0)}] + J_{12}[X, f_2^{(0)}]), \tag{42a}$$

$$\mathcal{M}_1 X = -J_{12}[f_2^{(0)}, X]. \tag{42b}$$

In equations (36)–(38), $\zeta^{(0)}$ and $P_{r,ij}^{(0)}$ are the zeroth-order approximations to the cooling rate and the partial pressure tensor, respectively, and $f_1^{(0)}$ is the zeroth-order distribution function.

4. Shear-rate dependent diffusion coefficients. Tracer limit

The generalized diffusion coefficients $D_{ij}, D_{p,ij}$, and $D_{T,ij}$ are nonlinear functions of the shear rate and the parameters of the mixture (masses, concentration and coefficients of restitution). In dimensionless form, the above coefficients can be written as

$$D_{ij} = \frac{\rho T}{m_1 m_2 \nu_0} D_{ij}^*, \tag{43}$$

$$D_{p,ij} = \frac{p}{\rho \nu_0} D_{p,ij}^*, \quad D_{T,ij} = \frac{p}{\rho \nu_0} D_{T,ij}^*. \tag{44}$$

In order to determine them, one has to multiply equations (36)–(38) by $m_1 c_j$ and integrate over **c**. After some algebra, the (scaled) diffusion coefficients D_{ij}^*, $D_{p,ij}^*$ and $D_{T,ij}^*$ obey the following set of coupled algebraic equations:

$$-(\lambda + \nu_D^*) D_{ij}^* - a_{ik}^* D_{kj}^* = \frac{\rho_1}{\rho} \frac{\partial P_{ij}^*}{\partial x_1} - \frac{\partial P_{1,ij}^*}{\partial x_1} + \frac{\partial \lambda}{\partial x_1} (D_{p,ij}^* + D_{T,ij}^*), \tag{45}$$

$$\left(2\lambda - a^* \frac{\partial \lambda}{\partial a^*} + \nu_D^*\right) D_{p,ij}^* + a_{ik}^* D_{p,kj}^* = -\left(\frac{\rho_1}{\rho} P_{ij}^* - P_{1,ij}^*\right) + \frac{\rho_1}{\rho} a^* \frac{\partial P_{ij}^*}{\partial a^*} - a^* \frac{\partial P_{1,ij}^*}{\partial a^*} - \left(\lambda - a^* \frac{\partial \lambda}{\partial a^*}\right) D_{T,ij}^*, \tag{46}$$

$$\left(a^* \frac{\partial \lambda}{\partial a^*} + \nu_D^*\right) D_{T,ij}^* + a_{ik}^* D_{T,kj}^* = -\frac{\rho_1}{\rho} a^* \frac{\partial P_{ij}^*}{\partial a^*} + a^* \frac{\partial P_{1,ij}^*}{\partial a^*} + \left(\lambda - a^* \frac{\partial \lambda}{\partial a^*}\right) D_{p,ij}^*. \tag{47}$$

In equations (45)–(47), we have introduced the dimensionless quantities $\zeta^* \equiv \zeta^{(0)}/\nu_0$, $P_{r,ij}^* \equiv P_{r,ij}^{(0)}/p$, $P_{ij}^* \equiv P_{ij}^{(0)}/p = P_{1,ij}^* + P_{2,ij}^*$ and

$$\nu_D^* = \frac{\rho \omega_{12}^*}{d\rho_2} \mu_{21}(1 + \alpha_{12}), \tag{48}$$

where $\omega_{12}^* \equiv \omega_{12}/\nu_0$. Upon deriving equations (45)–(47) use has been made of the result

$$a^* \frac{\partial \lambda}{\partial a^*} = -\frac{2a^*}{d}\left(P_{xy}^* + a^* \frac{\partial P_{xy}^*}{\partial a^*}\right) - a^* \frac{\partial \zeta^*}{\partial a^*}, \tag{49}$$

that comes from the identity

$$\lambda = -\left(\zeta^* + \frac{2a^*}{d} P_{xy}^*\right). \tag{50}$$

The solution to equations (45)–(47) provides the explicit forms of the set of diffusion coefficients for arbitrary concentration. In particular, in the absence of shear field ($a^* = 0$), $P_{ij}^* = \delta_{ij}$, $P_{r,ij}^* = x_r \gamma_r \delta_{ij}$, and so the tensorial quantities D_{ij}^*, $D_{p,ij}^*$ and $D_{T,ij}^*$ becomes scalar coefficients, namely, $D_{ij}^* = D^* \delta_{ij}$, $D_{p,ij}^* = D_p^* \delta_{ij}$ and $D_{T,ij}^* = D_T^* \delta_{ij}$ where

$$D^* = (\nu_D^* + \lambda)^{-1}\left[\frac{\partial}{\partial x_1}(x_1\gamma_1) - \frac{\partial\lambda}{\partial x_1}(D_p^* + D_T^*)\right], \tag{51}$$

$$D_p^* = x_1\gamma_1\left(1 - \frac{pm_1}{\rho T_1}\right)\left(\nu_D^* + 2\lambda + \frac{\lambda^2}{\nu_D^*}\right)^{-1}, \tag{52}$$

$$D_T^* = \frac{\lambda}{\nu_D^*}D_p^*. \tag{53}$$

The expressions (51)–(53) are consistent with those previously derived in the Navier–Stokes hydrodynamic order [11].

We now address the tracer limit ($x_1 \to 0$) for D_{ij}^*, $D_{p,ij}^*$ and $D_{T,ij}^*$. The analysis is quite delicate and shows that the above coefficients turn out to be qualitatively different in the disordered and ordered phase, as may have been expected from the previous results obtained in the Navier–Stokes order [20]. Let us consider each phase separately.

4.1. Disordered phase

In the disordered phase, $\lambda = \lambda_2^{(0)}$, the temperature ratio is finite and the energy ratio $p_1^* = 0$. Moreover, the results displayed in appendix A show that in the disordered phase $P_{1xy,\mathrm{dis}}^*$ and $P_{1yy,\mathrm{dis}}^*$ are proportional to x_1 and hence, they vanish in the tracer limit. On the other hand,

$$\lim_{x_1 \to 0}\left(\frac{\partial P_{1ij,\mathrm{dis}}^*}{\partial x_1}\right)_{p,T} = \mathcal{P}_{1ij,\mathrm{dis}}^{(1)}, \tag{54}$$

where the explicit forms of the relevant elements $\mathcal{P}_{1xy,\mathrm{dis}}^{(1)}$ and $\mathcal{P}_{1yy,\mathrm{dis}}^{(1)}$ are defined by equations (A.21) and (A.22), respectively. In these conditions, the set of equations (46) and (47) obeyed by the tensors $D_{p,ij}^*$ and $D_{T,ij}^*$ become a set of *homogeneous* equations whose solution yields $D_{p,ij}^* = D_{T,ij}^* = 0$. In the case of the diffusion tensor D_{ij}^*, equation (45) becomes

$$(\lambda_2^{(0)} + \nu_D^*)D_{ij}^* + a_{ik}^* D_{kj}^* = \mathcal{P}_{1ij,\mathrm{dis}}^{(1)}, \tag{55}$$

whose solution is

$$D_{ij}^* = \frac{1}{\lambda_2^{(0)} + \nu_D^*}\left(\delta_{ik} - \frac{a_{ik}^*}{\lambda_2^{(0)} + \nu_D^*}\right)\mathcal{P}_{1kj,\mathrm{dis}}^{(1)}. \tag{56}$$

Here, we have introduced the tensor $a_{k\ell}^* = a^*\delta_{kx}\delta_{\ell y}$ and $\nu_D^* = \mu_{21}(1 + \alpha_{12})/2$ in the tracer limit. Equation (56) was already obtained in [10] in the study of diffusion of impurities in a sheared inelastic Maxwell gas. Moreover, when $a^* = 0$, $\mathcal{P}_{1ij,\mathrm{dis}}^{(1)} = \gamma_1\delta_{ij}$ and one recovers the results derived in the Navier–Stokes approximation [11].

4.2. Ordered phase

The calculations in the ordered phase are, expectedly, more intricate. In this case, $\lambda = \lambda_1^{(0)}$, $\gamma_1 \to \infty$ but $p_1^{(0)} \equiv E_1/E \neq 0$. Here, $p_1^{(0)}$ is the zeroth-order contribution to the expansion of p_1^* in powers of the concentration x_1, i.e.

$$p_1^* = p_1^{(0)} + p_1^{(1)} x_1 + \dots . \tag{57}$$

In addition, in order to obtain the diffusion tensors, we need also to evaluate the two first terms of the expansion of the tracer pressure tensor $P_{1ij,\text{ord}}^*$ in powers of x_1:

$$P_{1ij,\text{ord}}^* = \mathcal{P}_{1ij,\text{ord}}^{(0)} + \mathcal{P}_{1ij,\text{ord}}^{(1)} x_1 + \dots . \tag{58}$$

The explicit expressions of $\mathcal{P}_{1ij,\text{ord}}^{(0)}$ and $\mathcal{P}_{1ij,\text{ord}}^{(1)}$ are provided in appendix A. Once these quantities are known, the set of coupled equations verified by the diffusion tensors in the ordered phase can be obtained after taking the tracer limit in equations (45)–(47). The result is

$$-(\lambda_1^{(0)} + \nu_D^*) D_{ij}^* - a_{ik}^* D_{kj}^* = -\mathcal{P}_{1ij,\text{ord}}^{(1)} + \lambda_1^{(1)} (D_{p,ij}^* + D_{T,ij}^*), \tag{59}$$

$$\left(2\lambda_1^{(0)} - a^* \frac{\partial \lambda_1^{(0)}}{\partial a^*} + \nu_D^* \right) D_{p,ij}^* + a_{ik}^* D_{p,kj}^* = \mathcal{P}_{1ij,\text{ord}}^{(0)} - a^* \frac{\partial \mathcal{P}_{1ij,\text{ord}}^{(0)}}{\partial a^*} - \left(\lambda_1^{(0)} - a^* \frac{\partial \lambda_1^{(0)}}{\partial a^*} \right) D_{T,ij}^*, \tag{60}$$

$$\left(2\lambda_1^{(0)} - a^* \frac{\partial \lambda_1^{(0)}}{\partial a^*} + \nu_D^* \right) D_{T,ij}^* + a_{ik}^* D_{T,kj}^* = a^* \frac{\partial \mathcal{P}_{1ij,\text{ord}}^{(0)}}{\partial a^*} + \left(\lambda_1^{(0)} - a^* \frac{\partial \lambda_1^{(0)}}{\partial a^*} \right) D_{p,ij}^*, \tag{61}$$

where the explicit expression of $\lambda_1^{(1)}$ is provided in appendix C of [18]. Equations (59)–(61) are the most relevant results of the present paper since their solution provides the dependence of D_{ij}^*, $D_{p,ij}^*$ and $D_{T,ij}^*$ on the parameters of the system in the ordered phase. In particular, once the set of coupled algebraic equations (60) and (61) for $D_{p,ij}^*$ and $D_{T,ij}^*$ are solved, the solution to equation (59) is simply

$$D_{ij}^* = \frac{1}{\lambda_1^{(0)} + \nu_D^*} \left(\delta_{ik} - \frac{a_{ik}^*}{\lambda_1^{(0)} + \nu_D^*} \right) [\mathcal{P}_{1kj,\text{ord}}^{(1)} - \lambda_1^{(1)} (D_{p,kj}^* + D_{T,kj}^*)] . \tag{62}$$

5. Some illustrative systems

The results derived in the previous section gives the dependence of the set of (scaled) diffusion coefficients $\mathcal{D}_{ij} \equiv \{D_{ij}^*, D_{p,ij}^*, D_{T,ij}^*\}$ in the disordered and ordered phases in terms of the mass ratio μ, the coefficients of restitution α_{12} and α_{22} and the dimensionality of the system d. Highly nonlinear functions on the above parameter space appear.

According to equations (56) and (59)–(61), $\mathcal{D}_{xz} = \mathcal{D}_{zx} = \mathcal{D}_{yz} = \mathcal{D}_{zy} = 0$ in agreement with the symmetry of the linear shear flow (15). Therefore, there are five relevant (nonzero) elements of the tensors $\mathcal{D}_{ij}$: the three diagonal ($\mathcal{D}_{xx}$, $\mathcal{D}_{yy}$ and $\mathcal{D}_{zz}$) and the
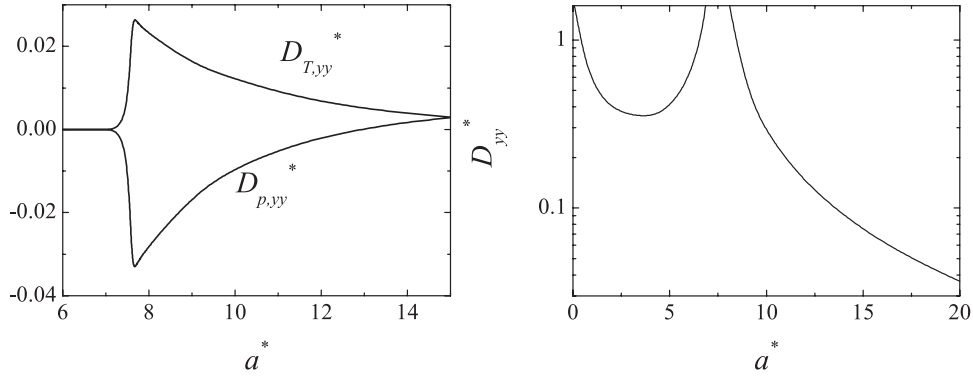
Figure 1. Shear rate dependence of the diffusion coefficients $D^*_{p,yy}$, $D^*_{T,yy}$ and D^*_{yy} for a three-dimensional system with a mass ratio $\mu = 0.2$ and a (common) coefficient of restitution $\alpha = \alpha_{22} = \alpha_{12} = 0.9$. In this case, the value of the critical shear rate a^*_c beyond which the ordered phase appears is $a^*_c \simeq 7.56$.

two off-diagonal elements ($\mathcal{D}_{xy}$ and $\mathcal{D}_{yx}$). Equations (56) and (59)–(61) also show that the anisotropy produced by the shear flow leads to the properties $\mathcal{D}_{xx} \neq \mathcal{D}_{yy} = \mathcal{D}_{zz}$ and $\mathcal{D}_{xy} \neq \mathcal{D}_{yx}$. Note that the equality $\mathcal{D}_{yy} = \mathcal{D}_{zz}$ is a consequence of the identity $P^*_{1,yy} = P^*_{1,zz}$. This property is due to the interaction model considered since $\mathcal{D}_{yy} \neq \mathcal{D}_{zz}$ for IHS [37, 38].

In order to illustrate the shear-rate dependence of those coefficients, we consider a three-dimensional system ($d = 3$) with a *common* coefficient of restitution ($\alpha \equiv \alpha_{22} = \alpha_{12}$). This reduces our parameter space to three independent quantities: μ, α and a^*. In this case (symmetric dissipation), according to equation (25), the value of the threshold mass ratio $\mu^{(-)}_{\text{th}}$ for the light impurity phase is independent of the coefficient of restitution, i.e. $\mu_{\text{th}} = \sqrt{2} - 1 \simeq 0.414$. Since this phase is also present in the elastic case [32], we focus our attention first onto a system with a mass ratio $\mu < \mu^{(-)}_{\text{th}}$. More specifically, we consider the mass ratio $\mu = 0.2$ for which the critical value of the (reduced) shear rate $a^*_c \simeq 7.56$ and so, the disordered phase exists for $a^* \gtrsim 7.56$.

Figures 1–4 are for the dependence of the coefficients $\mathcal{D}_{ij}$ for $\mu = 0.2$ and $\alpha = 0.9$. As expected, the results show that the coefficients $D^*_{p,ij}$ and $D^*_{T,ij}$ vanish in the disordered phase but they are different from zero in the ordered phase. The coefficients D^*_{ij} diverge in the disordered phase at the critical point (since $\mathcal{P}^{(1)}_{1ij,\text{dis}} \propto \gamma_1 \to \infty$), but remain finite in the ordered phase. In general, we observe that the effect of the shear flow on diffusion is quite significant, especially for the tracer diffusion coefficients D^*_{ij}.

We start our discussion with the diagonal terms $\mathcal{D}_{ii}$ ($i = x, y, z$). In the case of D^*_{yy} and D^*_{xx}, it appears that their shear-rate dependence is qualitatively similar in the ordered phase ($a^* > a^*_c$) since both coefficients decrease with increasing the shear rate. In the disordered phase however, while D^*_{yy} exhibits a non-monotonic dependence on a^*, D^*_{xx} increases with a^* and thus, shearing enhances diffusion along the x direction. In addition, at a more quantitative level, we also observe that the anisotropy of the system (as measured by the difference $D^*_{xx} - D^*_{yy}$) grows with the shear rate in the disordered phase while the opposite happens in the ordered phase (since for instance, $D^*_{xx} - D^*_{yy} \simeq 7.29$ at $a^* = 10$ and $D^*_{xx} - D^*_{yy} \simeq 4.13$ at $a^* = 12$). In any case, both diagonal elements (which can be understood as generalized mutual diffusion coefficients in a sheared mixture)
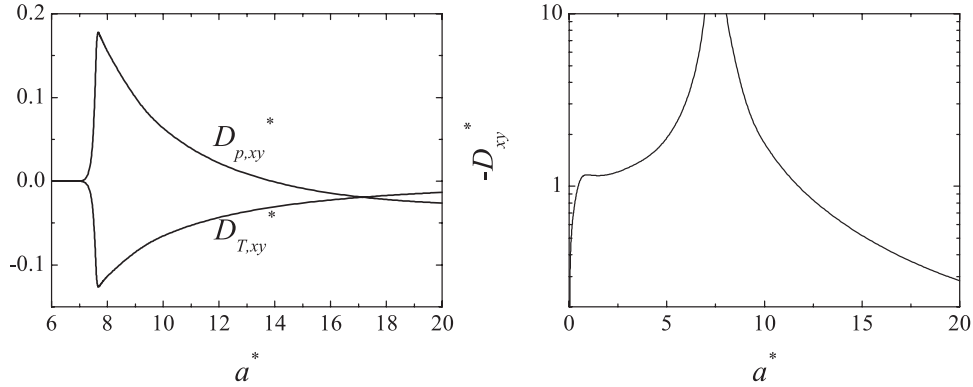
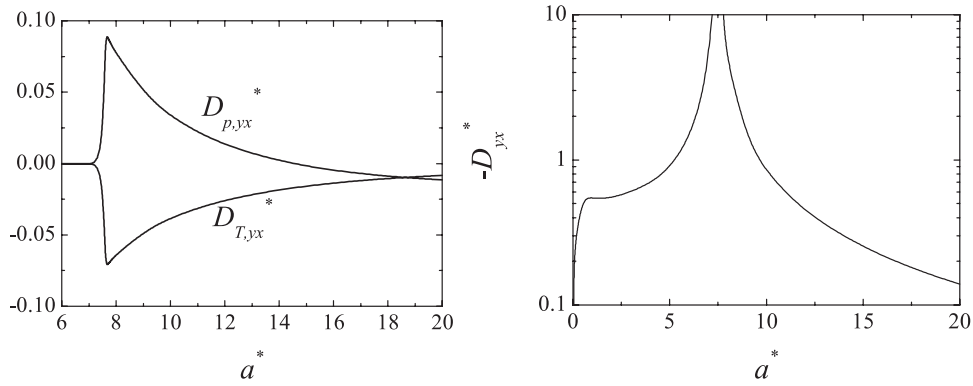**Figure 2.** Same as in figure 1 for the coefficients $D_{p,xy}^*$, $D_{T,xy}^*$ and $-D_{xy}^*$.

Figure 3. Same as in figure 1 but for the coefficients $D_{p,yx}^*$, $D_{T,yx}^*$ and $-D_{yx}^*$.
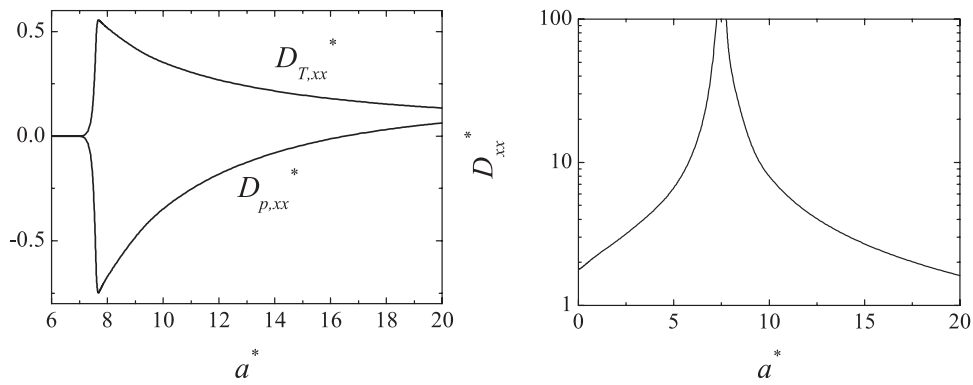

Figure 4. Same as in figure 1 but for the coefficients $D_{p,xx}^*$, $D_{T,xx}^*$ and D_{xx}^*.

tend to zero as the shear rate becomes large, this tendency being much slower in the case of D_{xx}^*. As far as the diagonal elements $D_{p,ii}^*$ and $D_{T,ii}^*$ are concerned, we see first that they can be positive or negative in the ordered phase, although their magnitude is much smaller than their counterparts D_{ii}^*. Moreover, $|D_{p,ii}^*|$ and $|D_{T,ii}^*|$ decrease with a^* and tend to vanish at large shear rates.

We consider now the off-diagonal elements $\mathcal{D}_{ij}$ $(i \neq j)$. They measure cross effects in the diffusion of particles induced by the shear flow. Thus, for instance, D_{xy}^* gives the
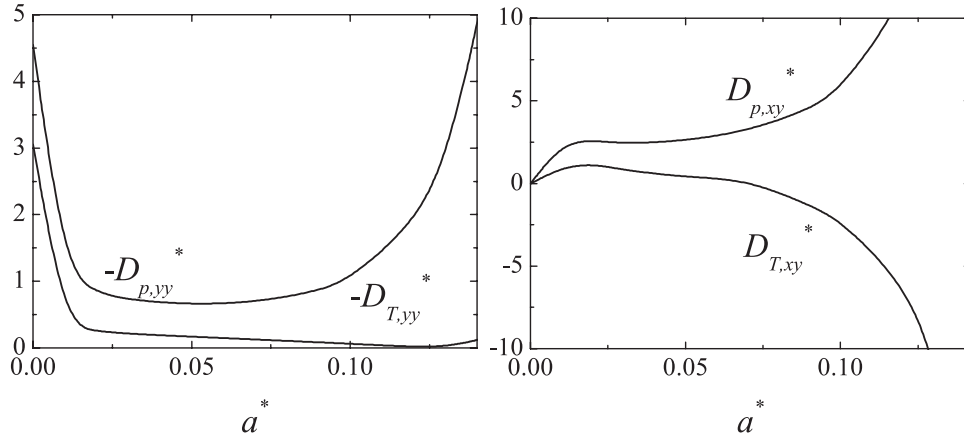
Figure 5. Shear rate dependence of $-D^*_{p,yy}$, $-D^*_{T,yy}$, $D^*_{p,xy}$ and $D^*_{T,xy}$ for a three-dimensional system with a mass ratio $\mu = 50$ and a (common) coefficient of restitution $\alpha = \alpha_{22} = \alpha_{12} = 0.9$. In this case, the ordered phase exists for $a^* < a^{*(+)} \simeq 0.142$. On the other hand, in the disordered region ($a^* > 0.142$), all quantities plotted vanish.
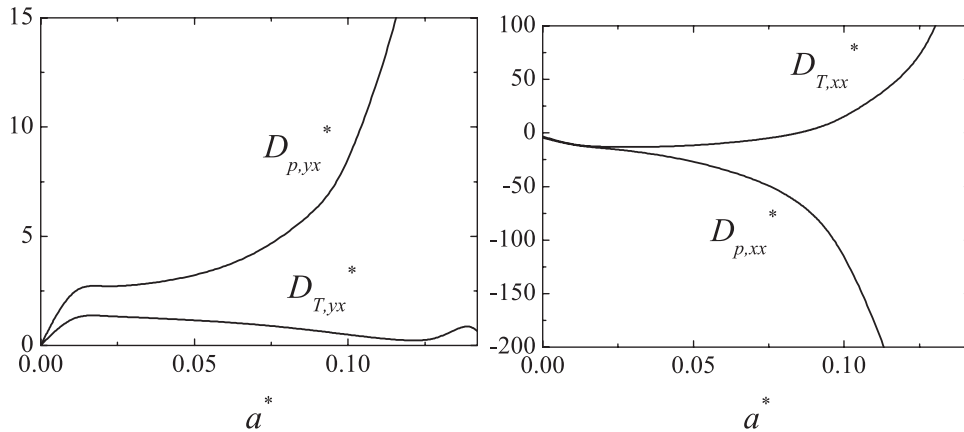

Figure 6. Same as in figure 5 but for the coefficients $D^*_{p,yx}$, $D^*_{T,yx}$, $D^*_{p,xx}$ and $D^*_{T,xx}$.

transport of mass along the direction of the flow (x axis) due to a concentration gradient parallel to the gradient of the flow velocity (y axis). While D^*_{xy} and D^*_{yx} are negative, a different behaviour is reported for the coefficients $D^*_{p,ij}$ and $D^*_{T,ij}$ (with $i \neq j$). As in the case of the diagonal elements, the magnitude of the latter coefficients is in general smaller than that of the cross-coefficients D^*_{xy} and D^*_{yx}. We also observe that the shear-rate dependence of $|D^*_{xy}|$ and $|D^*_{yx}|$ is quite similar in both phases for the system parameters chosen in figures 2 and 3: they first display a non-monotonic dependence on a^* in the disordered phase, then tend to infinity at the critical point while they decrease upon increasing the shear rate in the ordered phase. As for the diagonal elements, $|D^*_{xy}|$ is in general larger than $|D^*_{yx}|$ showing that the coupling between the shear field and the concentration gradient enhances significantly the mass transport along the direction of the flow. Finally, it must noted that the behaviour of $D^*_{p,ij}$ and $D^*_{T,ij}$ (with $i \neq j$) is quite similar to that of the diagonal elements since they vanish in the disordered phase and then their magnitude decreases as the shear rate increases.

17

Now, we consider a situation where the ordered phase appears for heavy impurities. For symmetric dissipation, this phase exists for $\mu > \mu_{\text{HCS}}^{(+)}$ (where $\mu_{\text{HCS}}^{(+)}$ is given by the second identity of equation (26)) and $a^* < a^{*(+)}$ (where $a^{*(+)}$ is given by equation (27)). For $d = 3$ and $\alpha = \alpha_{22} = \alpha_{12} = 0.9$, $\mu_{\text{HCS}}^{(+)} \simeq 38.03$ and $a^{*(+)} \simeq 0.142$. Figures 5 and 6 show the shear-rate dependence of the relevant elements of the tensors $D_{p,ij}^*$ and $D_{T,ij}^*$. The mutual diffusion tensor D_{ij}^* has not been plotted since in the ordered region the conventional diffusion coefficient D^* (defined by equation (51)) yields unphysical negative values ($D^* < 0$) when one considers the 'vanilla' version of the inelastic Maxwell model. This drawback of the model was already discussed in [20], where it was found that the kinetic theory calculations disagree with Monte Carlo simulations: the latter predict that the coefficient D^* (which can be understood as the vanishing shear rate limit of the tensor D_{ij}^*) diverges in the ordered phase while theoretical predictions yield finite values. It appears from figures 5 and 6 that the impact of shear flow on $D_{p,ij}^*$ and $D_{T,ij}^*$ is more important here than in the light impurity phase case. This could come as a surprise since the magnitude of shear rates covering the ordered heavy tracer region is smaller than that of the corresponding ordered light tracer region. However, it seems that the effect of the mass ratio on diffusion (with relatively small shear rates) in the present case (Brownian limit) is more significant than the effect of the shear rate on diffusion (with relatively large shear rates) when the tracer particles are lighter than the gas particles. Thus, in particular, there is a significant enhancement of the magnitude of the coefficients $D_{p,xx}^*$ and $D_{T,xx}^*$ with respect to their vanishing shear rate values D_p^* (defined by equation (52)) and D_T^* (defined by equation (53)), respectively.

6. Discussion

In this paper, we have analyzed the effects of a recent non-equilibrium transition [17, 18] found for inelastic Maxwell models when the concentration of one of the species x_1 of a binary mixture is negligible (tracer limit). The emphasis was put on the diffusion coefficients of impurities immersed in a strongly sheared granular gas. In this transition, at given values of the shear rate and the parameters of the system (masses and coefficients of restitution for collisions between tracer and gas particles and gas particles among themselves), there are regions (coined as ordered phases) where quite surprisingly the relative contribution of the tracer species to the total properties of the mixture does not vanish as $x_1 \to 0$. Two families of ordered phase appear: (i) a light impurity phase which exists when the mass ratio $\mu \equiv m_1/m_2$ does not exceed the threshold value $\mu_{\text{th}}^{(-)}$ (defined by equation (25)) and the shear rate is larger than a certain critical value, and (ii) a heavy impurity phase which appears when $\mu > \mu_{\text{HCS}}^{(+)}$ (defined by the second identity of equation (26)) and shear rates smaller than $a^{*(+)}$ (defined by equation (27)). The light impurity phase can also exist at $a^* = 0$ when $\alpha_{12} > \sqrt{(1 + \alpha_{22})^2/2}$. While the light impurity phase was already found [32] in the case of ordinary (elastic) mixtures, the second one (heavy impurity phase) is absent for elastic collisions since $a^{*(+)} = 0$ when $\alpha_{22} = 1$. It must be noted that both light and heavy ordered phases disappear when $a^* < a_c^*$ and $\mu < \mu_{\text{HCS}}^{(+)}$ in the particular case of symmetric dissipation ($\alpha_{12} = \alpha_{22}$).

As expected, in the disordered phase, the properties of the mixture coincide with that of the excess gas.

Because of the anisotropy induced by the shear flow, tensorial quantities are required to describe mass transport. Thus, the mass flux $j_1^{(1)}$ of impurities is given by equation (32) where the second-rank (scaled) tensors D_{ij}^*, $D_{p,ij}^*$ and $D_{T,ij}^*$ obey the set of coupled algebraic equations (45)–(47) for arbitrary concentration ($x_1 \neq 0$). Starting from these general equations, the forms of those shear-rate dependent tensors have been explicitly obtained in both disordered and ordered phases, by enforcing carefully the tracer limit. It was found that the dependence of the (scaled) diffusion coefficients on both the (reduced) shear rate a^* and the parameters of the mixture (mass ratio μ and the coefficients of restitution α_{22} and α_{12}) is clearly different in both phases. The pressure $D_{p,ij}^*$ and thermal $D_{T,ij}^*$ diffusion coefficients vanish in the disordered phase while they are given by equations (60) and (61), respectively, in the ordered phase. The expression of the mutual diffusion coefficients D_{ij}^*, for the disordered phase, coincides with the one derived before [10] by starting from the Boltzmann–Lorentz equation for the tracer particles. On the other hand, it is given by equation (62) in the ordered phase.

The results show that in general the shear-rate dependence of all the coefficients is quite complex. In particular, as happens in the Navier–Stokes description [20], only the mutual diffusion coefficients D_{ij}^* diverge at the critical point. Moreover, the analysis carried out in section 4 shows that D_{ij}^* turns out negative in the ordered heavy tracer phase for all the range of shear rates studied. Since the diagonal elements of this tensor can be seen as a generalization of the mutual diffusion coefficient D^* (defined by equation (51)), one could expect that these elements should be positive. The fact that D_{ii}^* is negative for $a^* < a^{*(+)}$ could be a reminiscence of the unphysical behaviour found for D^* in the ordered phase for extreme values of the mass ratio [20]. In addition, given that significant discrepancies were found in [20] for the tracer diffusion between theory and Monte Carlo simulations in the ordered phase, a possible scenario to explain this disagreement could be the breakdown of hydrodynamics in the ordered phase for large mass ratios. On the other hand, beyond this region, the present results for the set of shear-rate dependent coefficients show that all of them are well behaved and so, one could speculate that granular hydrodynamics (in the sense that all the space and time dependence of the distribution functions occurs entirely through a functional dependence on the hydrodynamic fields) is here valid. A complete answer to this question would require additional numerical work to measure some of these coefficients. We plan to perform Monte Carlo simulations in a sheared granular mixture by following the strategy adopted years ago by Campbell [39] who computed the self-diffusion tensor via molecular-dynamics simulations, using particle tracking and through velocity correlations.

Acknowledgments

Appendix A. Expressions of the partial pressure tensors in the USF state

In this appendix, we display the explicit forms of the (reduced) pressure tensors $P^*_{r,ij}$ ($r = 1, 2$) in the USF state for arbitrary concentration ($x_1 \neq 0$). First, the (global) shear stress P^*_{xy} is given by $P^*_{xy} = P^*_{1,xy} + P^*_{2,xy}$ where

$$P^*_{1,xy} = \frac{d}{2a^*}\left[A^*_{12} - B^*_{12} - (B^*_{11} + \lambda - A^*_{11} + A^*_{12} - B^*_{12})p^*_1\right], \tag{A.1}$$

$$P^*_{2,xy} = \frac{d}{2a^*}\left[A^*_{21} - B^*_{21} - (B^*_{22} + \lambda - A^*_{22} + A^*_{21} - B^*_{21})(1 - p^*_1)\right]. \tag{A.2}$$

Here,

$$A^*_{11} = \frac{\omega^*_{11}}{2(d+2)}(1 + \alpha_{11})^2 + \frac{\omega^*_{12}}{d+2}\mu^2_{21}(1 + \alpha_{12})^2, \tag{A.3}$$

$$A^*_{12} = \frac{\omega^*_{12}}{d+2}\frac{\rho_1}{\rho_2}\mu^2_{21}(1 + \alpha_{12})^2, \tag{A.4}$$

$$B^*_{11} = \frac{\omega^*_{11}}{d(d+2)}(1 + \alpha_{11})(d + 1 - \alpha_{11}) + \frac{2\omega^*_{12}}{d(d+2)}\mu_{21}(1 + \alpha_{12})\left[d + 2 - \mu_{21}(1 + \alpha_{12})\right], \tag{A.5}$$

$$B^*_{12} = -\frac{2}{d}A^*_{12}, \tag{A.6}$$

where $\omega^*_{rs} = \omega^*_{rs}/\nu_0$. Adequate change of indices ($1 \leftrightarrow 2$) provide the equations pertaining to A^*_{22}, A^*_{21}, B^*_{22}, and B^*_{21}. In addition, in equations (A.1) and (A.2) the energy ratio p^*_1 can be written as [18]

$$p^*_1 = \frac{Ka^{*2} + L}{Ra^{*2} + S}, \tag{A.7}$$

where

$$K = -2A^*_{12}\lambda^2 + 4(A^*_{22}B^*_{12} - A^*_{12}B^*_{22})\lambda + 2A^*_{22}B^*_{12}(B^*_{11} + B^*_{22}) - 2A^*_{12}(B^*_{12}B^*_{21} + B^{*2}_{22}), \tag{A.8}$$

$$L = d(B^*_{12} - A^*_{12})[\lambda^2 + (B^*_{11} + B^*_{22})\lambda + B^*_{11}B^*_{22} - B^*_{12}B^*_{21}]^2, \tag{A.9}$$

$$R = 2(A^*_{11} - A^*_{12})\lambda^2 - 4[B^*_{12}(A^*_{21} - A^*_{22}) + B^*_{22}(A^*_{12} - A^*_{11})]\lambda$$
$$+ 2B^*_{12}(B^*_{11} + B^*_{22})(A^*_{22} - A^*_{21}) + 2(A^*_{11} - A^*_{12})(B^*_{12}B^*_{21} + B^{*2}_{22}), \tag{A.10}$$

$$S = d(A^*_{11} - A^*_{12} - B^*_{11} + B^*_{12} - \lambda)[\lambda^2 + (B^*_{11} + B^*_{22})\lambda + B^*_{11}B^*_{22} - B^*_{12}B^*_{21}]^2. \tag{A.11}$$

The other relevant element of the pressure tensor is $P^*_{yy} = P^*_{zz}$. It is given by $P^*_{yy} = P^*_{1,yy} + P^*_{2,yy}$ where

$$P^*_{1,yy} = P^*_{1,zz} = \frac{(B^*_{22} + \lambda)\,[\,p^*_1 A^*_{11} + (1 - p^*_1)A^*_{12}] - B^*_{12}\,[\,p^*_1 A^*_{21} + (1 - p^*_1)A^*_{22}]}{(B^*_{11} + \lambda)(B^*_{22} + \lambda) - B^*_{12}B^*_{21}}, \tag{A.12}$$

$$P^*_{2,yy} = P^*_{2,zz} = \frac{(B^*_{11} + \lambda)\,[\,p^*_1 A^*_{21} + (1 - p^*_1)A^*_{22}] - B^*_{21}\,[\,p^*_1 A^*_{11} + (1 - p^*_1)A^*_{12}]}{(B^*_{11} + \lambda)(B^*_{22} + \lambda) - B^*_{12}B^*_{21}}. \tag{A.13}$$

Finally, the xx-element $P^*_{xx} = P^*_{1,xx} + P^*_{2,xx}$ where its partial contributions can be easily determined from the constraint

$$P^*_{r,xx} = dx_r\gamma_r - (d-1)P^*_{r,yy}, \tag{A.14}$$

where $\gamma_r \equiv T_r/T$ is the partial temperature of species r.

The above expressions for the partial contributions $P^*_{r,ij}$ to the pressure tensor hold for arbitrary values of x_1. Let us consider now the forms of $P^*_{r,ij}$ in the tracer limit ($x_1 \to 0$). In this case, we assume that $P^*_{r,ij}$ and p^*_1 can be expanded as

$$P^*_{r,ij} = \mathcal{P}^{(0)}_{r,ij} + \mathcal{P}^{(1)}_{r,ij}x_1 + \mathcal{P}^{(2)}_{r,ij}x_1^2 + \dots, \tag{A.15}$$

$$p^*_1 = p^{(0)}_1 + p^{(1)}_1 x_1 + p^{(2)}_1 x_1^2 + \dots. \tag{A.16}$$

The expressions of $\mathcal{P}^{(k)}_{r,ij}$ and $p^{(k)}_1$ will be different if $\lambda^{(0)}_2 > \lambda^{(0)}_1$ (disordered phase) or $\lambda^{(0)}_1 > \lambda^{(0)}_2$ (ordered phase). In particular, in the lowest order in x_1, the expressions of $\mathcal{P}^{(0)}_{r,ij}$ in the disordered phase are simply $\mathcal{P}^{(0)}_{1xy,\mathrm{dis}} = \mathcal{P}^{(0)}_{1yy,\mathrm{dis}} = 0$,

$$\mathcal{P}^{(0)}_{2xy,\mathrm{dis}} = -\frac{A^{(0)}_{22}}{(B^{(0)}_{22} + \lambda^{(0)}_2)^2}\,a^*, \tag{A.17}$$

$$\mathcal{P}^{(0)}_{2yy,\mathrm{dis}} = \frac{A^{(0)}_{22}}{B^{(0)}_{22} + \lambda^{(0)}_2}, \tag{A.18}$$

where

$$A^{(0)}_{22} = \frac{(1 + \alpha_{22})^2}{2(d+2)}, \tag{A.19}$$

$$B^{(0)}_{22} = \frac{(1 + \alpha_{22})(d + 1 - \alpha_{22})}{d(d+2)}, \tag{A.20}$$

and use has been made of the fact that $p^{(0)}_1 = 0$ in the disordered phase. In addition, to get the (reduced) diffusion tensor D^*_{ij} in the disordered phase, we need the expressions of $\mathcal{P}^{(1)}_{1xy,\mathrm{dis}}$ and $\mathcal{P}^{(1)}_{1yy,\mathrm{dis}}$. They are given by

$$\mathcal{P}_{1xy,\mathrm{dis}}^{(1)} = \frac{d}{2a^*}\left[A_{12}^{(1)} - B_{12}^{(1)} + (A_{11}^{(0)} - B_{11}^{(0)} - \lambda_2^{(0)})\gamma_1\right], \tag{A.21}$$

$$\mathcal{P}_{1yy,\mathrm{dis}}^{(1)} = \frac{(B_{22}^{(0)} + \lambda_2^{(0)})(A_{11}^{(0)}\gamma_1 + A_{12}^{(1)}) - A_{22}^{(0)}B_{12}^{(1)}}{(B_{11}^{(0)} + \lambda_2^{(0)})(B_{22}^{(0)} + \lambda_2^{(0)})}, \tag{A.22}$$

where

$$A_{11}^{(0)} = \frac{\mu_{21}^2}{d+2}(1 + \alpha_{12})^2, \tag{A.23}$$

$$B_{11}^{(0)} = \frac{2}{d(d+2)}\mu_{21}(1 + \alpha_{12})\left[d + 2 - \mu_{21}(1 + \alpha_{12})\right], \tag{A.24}$$

$$A_{12}^{(1)} = \frac{\mu_{12}\mu_{21}}{(d+2)}(1 + \alpha_{12})^2, \tag{A.25}$$

$$B_{12}^{(1)} = -\frac{2}{d}A_{12}^{(1)}. \tag{A.26}$$

On the other hand, the temperature ratio $\gamma_1 = T_1/T$ is, in the tracer limit,

$$\gamma_1 = \frac{D_1(\lambda_2^{(0)})}{\Delta_0(\lambda_2^{(0)})}, \tag{A.27}$$

where the functions $D_1(\lambda)$ and $\Delta_0(\lambda)$ are given by

$$\begin{aligned} D_1(\lambda) = &\, d(B_{12}^{(1)} - A_{12}^{(1)})(B_{11}^{(0)} + \lambda)^2(B_{22}^{(0)} + \lambda)^2 \\ &+ 2a^{*2}[A_{22}^{(0)}B_{12}^{(1)}(B_{11}^{(0)} + B_{22}^{(0)} + 2\lambda) - A_{12}^{(1)}(B_{22}^{(0)} + \lambda)^2], \end{aligned} \tag{A.28}$$

$$\Delta_0(\lambda) = (B_{22}^{(0)} + \lambda)^2\left[2a^{*2}A_{11}^{(0)} + d(A_{11}^{(0)} - B_{11}^{(0)} - \lambda)(B_{11}^{(0)} + \lambda)^2\right]. \tag{A.29}$$

The quantities $\mathcal{P}_{1xx,\mathrm{dis}}^{(0)}$ and $\mathcal{P}_{1xx,\mathrm{dis}}^{(1)}$ can be easily identified from the relation (A.14) with the result

$$\mathcal{P}_{1xx,\mathrm{dis}}^{(0)} = -(d-1)\mathcal{P}_{1yy,\mathrm{dis}}^{(0)}, \tag{A.30}$$

$$\mathcal{P}_{1xx,\mathrm{dis}}^{(1)} = d\gamma_1 - (d-1)\mathcal{P}_{1yy,\mathrm{dis}}^{(1)}. \tag{A.31}$$

In the ordered phase, the zeroth-order expressions for the elements of the tracer pressure tensor $P_{1,ij}^*$ are

$$\mathcal{P}_{1xy,\mathrm{ord}}^{(0)} = \frac{d}{2a^*}(A_{11}^{(0)} - B_{11}^{(0)} - \lambda_1^{(0)})p_1^{(0)}, \tag{A.32}$$

$$\mathcal{P}_{1yy,\text{ord}}^{(0)} = \frac{A_{11}^{(0)}}{B_{11}^{(0)} + \lambda_1^{(0)}} p_1^{(0)}, \tag{A.33}$$

where

$$A_{21}^{(0)} = A_{12}^{(1)} = \frac{\mu_{12}\mu_{21}}{(d+2)}(1 + \alpha_{12})^2, \quad B_{21}^{(0)} = B_{12}^{(1)} = -\frac{2}{d}A_{21}^{(0)}, \tag{A.34}$$

$$A_{11}^{(1)} = \frac{1}{2(d+2)}(1 + \alpha_{11})^2 - A_{11}^{(0)}, \tag{A.35}$$

$$B_{11}^{(1)} = \frac{1}{d(d+2)}(1 + \alpha_{11})(d + 1 - \alpha_{11}) - B_{11}^{(0)}, \tag{A.36}$$

$$B_{22}^{(1)} = \frac{2}{d(d+2)}\mu_{12}(1 + \alpha_{12})\left[d + 2 - \mu_{12}(1 + \alpha_{12})\right] - B_{22}^{(0)}, \tag{A.37}$$

$$A_{22}^{(1)} = \frac{\mu_{21}^2}{d+2}(1 + \alpha_{12})^2 - A_{22}^{(0)}. \tag{A.38}$$

The zeroth-order contribution $p_1^{(0)}$ to the energy ratio is [18]

$$p_1^{(0)} = \frac{D_1(\lambda_1^{(0)})}{\Delta_0'(\lambda_1^{(0)})\lambda_1^{(1)} + \Delta_1(\lambda_1^{(0)})}, \tag{A.39}$$

where

$$\Delta_0'(\lambda_1^{(0)}) \equiv \left(\frac{\partial \Delta_0(\lambda)}{\partial \lambda}\right)_{\lambda = \lambda_1^{(0)}}, \tag{A.40}$$

and the expression of $\lambda_1^{(1)}$ is given by equations (C8)–(C13) of [18].

The first-order corrections $\mathcal{P}_{1xy,\text{ord}}^{(1)}$ and $\mathcal{P}_{1yy,\text{ord}}^{(1)}$ are also needed to determine the diffusion coefficients D_{ij}^* in the ordered phase. Their evaluation is quite involved and can be obtained by expanding the expressions (A.1) and (A.12) up to first order in x_1. After some algebra, one gets

$$\mathcal{P}_{1xy,\text{ord}}^{(1)} = \frac{d}{2a^*}\left[A_{12}^{(1)} - B_{12}^{(1)} - (B_{11}^{(1)} + \lambda_1^{(1)} - A_{11}^{(1)} + A_{12}^{(1)} - B_{12}^{(1)})p_1^{(0)} - (B_{11}^{(0)} + \lambda_1^{(0)} - A_{11}^{(0)})p_1^{(1)}\right], \tag{A.41}$$

$$\mathcal{P}_{1yy,\text{ord}}^{(1)} = \frac{1}{(B_{11}^{(0)} + \lambda_1^{(0)})^2(B_{22}^{(0)} + \lambda_1^{(0)})}\{(A_{12}^{(1)}(1 - p_1^{(0)}) + A_{11}^{(1)}p_1^{(0)} + A_{11}^{(0)}p_1^{(1)})(B_{11}^{(0)} + \lambda_1^{(0)})(B_{22}^{(0)} + \lambda_1^{(0)})$$
$$+ (B_{11}^{(0)} + \lambda_1^{(0)})[A_{11}^{(0)}p_1^{(0)}(B_{22}^{(1)} + \lambda_1^{(1)}) - B_{12}^{(1)}(A_{22}^{(0)}(1 - p_1^{(0)}) + A_{21}^{(0)}p_1^{(0)})]$$
$$- A_{11}^{(0)}p_1^{(0)}[(B_{11}^{(1)} + \lambda_1^{(1)})(B_{22}^{(0)} + \lambda_1^{(0)}) + (B_{11}^{(0)} + \lambda_1^{(0)})(B_{22}^{(1)} + \lambda_1^{(1)}) - B_{21}^{(0)}B_{12}^{(1)}]\}. \tag{A.42}$$

The explicit form of the first-order correction $p_1^{(1)}$ to the energy ratio is displayed in appendix B. Finally, the quantities $\mathcal{P}_{1xx,\mathrm{ord}}^{(0)}$ and $\mathcal{P}_{1xx,\mathrm{ord}}^{(1)}$ are defined as

$$\mathcal{P}_{1xx,\mathrm{ord}}^{(0)} = d\,p_1^{(0)} - (d-1)\mathcal{P}_{1yy,\mathrm{ord}}^{(0)}, \tag{A.43}$$

$$\mathcal{P}_{1xx,\mathrm{ord}}^{(1)} = d\,p_1^{(1)} - (d-1)\mathcal{P}_{1yy,\mathrm{ord}}^{(1)}. \tag{A.44}$$

Appendix B. First-order correction to the energy ratio

In the general case ($x_1 \neq 0$), the energy ratio p_1^* is given by equation (A.7). In the tracer limit ($x_1 \to 0$), p_1^* can be expanded in powers of x_1 as in equation (A.16) and $p_1^{(0)}$ is defined by equation (A.39). In this appendix, we want to get its first-order correction $p_1^{(1)}$. If $x_1 \to 0$, the energy ratio p_1^* becomes

$$p_1^*(\lambda, a^*) \approx x_1 \frac{D_1(\lambda, a^*) + D_2(\lambda, a^*)x_1}{\Delta_0(\lambda, a^*) + \Delta_1(\lambda, a^*)x_1 + \Delta_2(\lambda, a^*)x_1^2}, \tag{B.1}$$

where the dependence on μ, α_{11}, α_{22}, and α_{12} is implicitly assumed on the right-hand side of equation (B.1). The expressions of D_1 and Δ_0 are given by equations (A.28) and (A.29), respectively, while D_2, Δ_1 and Δ_2 can be easily obtained from the general form of p_1^*. Their explicit expressions are too cumbersome to be provided here and will be omitted[6]. Equation (B.1) applies for λ_1 and λ_2. The expansion of λ_1 in powers of x_1 can be written as

$$\lambda_1(a^*, x_1) \approx \lambda_1^{(0)}(a^*) + \lambda_1^{(1)}(a^*)x_1 + \lambda_1^{(2)}(a^*)x_1^2, \tag{B.2}$$

where the quantities $\lambda_1^{(1)}(a^*)$ and $\lambda_1^{(2)}(a^*)$ can be obtained from the sixth-degree polynomial equation defining λ in the USF problem [18]. As said before, the expression of $\lambda_1^{(1)}$ is given by equations (C8)–(C13) of [18]. On the other hand, the expression of $\lambda_1^{(2)}(a^*)$ is also too large to be displayed here.

The form of $p_1^{(1)}$ can be obtained by taking the tracer limit in equation (B.1). After some algebra, one arrives at

$$p_1^{(1)} = \frac{p_1^{(0)}}{D_1(\lambda_1^{(0)})}\left[D_2(\lambda_1^{(0)}) + D_1'(\lambda_1^{(0)})\lambda_1^{(1)} - p_1^{(0)}\left(\Delta_2(\lambda_1^{(0)}) + \Delta_0'(\lambda_1^{(0)})\lambda_1^{(2)} + \Delta_1'(\lambda_1^{(0)})\lambda_1^{(1)} + \frac{1}{2}\Delta_0''(\lambda_1^{(0)})\lambda_1^{(1)2}\right)\right], \tag{B.3}$$

where

$$D_1'(\lambda_1^{(0)}) \equiv \left(\frac{\partial D_1(\lambda)}{\partial \lambda}\right)_{\lambda=\lambda_1^{(0)}}, \quad \Delta_1'(\lambda_1^{(0)}) \equiv \left(\frac{\partial \Delta_1(\lambda)}{\partial \lambda}\right)_{\lambda=\lambda_1^{(0)}}, \quad \Delta_0''(\lambda_1^{(0)}) \equiv \left(\frac{\partial^2 \Delta_0(\lambda)}{\partial \lambda^2}\right)_{\lambda=\lambda_1^{(0)}}. \tag{B.4}$$

---

[6] See supplementary material for a Mathematica code that evaluates all the diffusion coefficients in the tracer limit for both ordered and disordered phases as functions of the mass ratio m_1/m_2 and the coefficients of restitution α_{12} and α_{22} (stacks.iop.org/JSTAT/2016/073206/mmedia).

In the absence of shear ($a^* = 0$), the expression (B.3) for $p_1^{(1)}$ reduces to the one previously derived in the homogeneous cooling state [20]. This shows the consistency of our results.

References

[1] Brilliantov N and Pöschel T 2004 *Kinetic Theory of Granular Gases* (Oxford: Clarendon)
[2] Puglisi A 2014 *Transport and Fluctuations in Granular Fluids: from Boltzmann Equation to Hydrodynamics, Diffusion and Motor Effects* (Heidelberg: Springer)
[3] Brey J J, Dufty J W, Kim C S and Santos A 1998 *Phys. Rev.* E **58** 4638
Garzó V and Dufty J W 1999 *Phys. Rev.* E **59** 5895
Garzó V, Hrenya C M and Dufty J W 2007 *Phys. Rev.* E **76** 031303
[4] Ernst M H 1981 *Phys. Rep.* **78** 1
[5] Truesdell C and Muncaster R G 1980 *Fundamentals of Maxwell's Kinetic Theory of a Simple Monatomic Gas* (New York: Academic)
[6] Garzó V and Santos A 2003 *Kinetic Theory of Gases in Shear Flows. Nonlinear Transport* (Dordrecht: Kluwer)
[7] Loose W and Hess S 1987 *Phys. Rev. Lett.* **58** 2443
Loose W 1988 *Phys. Lett.* A **128** 39
Gómez Ordoñez J, Brey J J and Santos A 1989 *Phys. Rev.* A **39** 3038
[8] Bobylev A V, Carrillo J A and Gamba I M 2000 *J. Stat. Phys.* **98** 743
Carrillo J A, Cercignani C and Gamba I M 2000 *Phys. Rev.* E **61** 7700
Ben-Naim E and Krapivsky P L 2000 *Phys. Rev.* E **61** R5
Cercignani C 2001 *J. Stat. Phys.* **102** 1407
Ernst M H and Brito R 2002 *J. Stat. Phys.* **109** 407
Ben-Naim E and Krapivsky P L 2003 *Granular Gas Dynamics* (*Lecture Notes in Physics* vol 624) ed T Pöschel and N Brilliantov (Berlin: Springer) pp 65–94
[9] Santos A 2003 *Physica* A **321** 442
[10] Garzó V 2003 *J. Stat. Phys.* **112** 657
[11] Garzó V and Astillero A 2005 *J. Stat. Phys.* **118** 935
[12] Santos A and Garzó V 2007 *J. Stat. Mech.* P08021
[13] Chamorro M G, Garzó V and Vega Reyes F 2014 *J. Stat. Mech.* P06008
[14] Ernst M H, Trizac E and Barrat A 2006 *J. Stat. Phys.* **124** 549
Ernst M H, Trizac E and Barrat A 2006 *Europhys. Lett.* **76** 56
[15] Kohlstedt K, Snezhko A, Sapozhnikov M V, Arnarson I S, Olafsen J S and Ben-Naim E 2005 *Phys. Rev. Lett.* **95** 068001
[16] Garzó V and Trizac E 2010 *J. Non-Newton. Fluid Mech.* **165** 932
[17] Garzó V and Trizac E 2011 *Europhys. Lett.* **94** 50009
[18] Garzó V and Trizac E 2012 *Phys. Rev.* E **84** 012301
[19] Garzó V and Trizac E 2012 *Granular Matter* **14** 99
[20] Garzó V, Khalil N and Trizac E 2015 *Eur. Phys. J.* E **38** 16
[21] Chapman S and Cowling T G 1970 *The Mathematical Theory of Nonuniform Gases* (Cambridge: Cambridge University Press)
[22] Garzó V and Trizac E 2015 *Phys. Rev.* E **92** 052202
[23] Marconi U M B and Puglisi A 2002 *Phys. Rev.* E **65** 051305
Marconi U M B and Puglisi A 2002 *Phys. Rev.* E **66** 011301
[24] Ben-Naim E and Krapivsky P L 2002 *Eur. Phys. J.* E **8** 507
[25] Montanero J M and Garzó V 2002 *Granular Matter* **4** 17
Barrat A and Trizac E 2002 *Granular Matter* **4** 57
Barrat A and Trizac E 2002 *Phys. Rev.* E **66** 051303
Dahl S R, Hrenya C M, Garzó V and Dufty J W 2002 *Phys. Rev.* E **66** 041301
Pagnani R, Marconi U M B and Puglisi A 2002 *Phys. Rev.* E **66** 051304
Krouskop P and Talbot J 2003 *Phys. Rev.* E **68** 021304
Wang H, Jin G and Ma Y 2003 *Phys. Rev.* E **68** 031301
[26] Wildman R D and Parker D J 2002 *Phys. Rev. Lett.* **88** 064301
[27] Feitosa K and Menon N 2002 *Phys. Rev. Lett.* **88** 198301
[28] Jenkins J and Mancini F 1987 *J. Appl. Mech.* **54** 27

[29] Garzó V and Dufty J W 1999 *Phys. Rev.* E **60** 5706
[30] Lees A W and Edwards S F 1972 *J. Phys. C: Solid State Phys.* **5** 1921
[31] Dufty J W, Santos A, Brey J J and Rodríguez R F 1986 *Phys. Rev.* A **33** 459
[32] Marín C, Santos A and Garzó V 1996 *Europhys. Lett.* **33** 599
[33] Lutsko J F 2006 *Phys. Rev.* E **73** 021302
[34] Garzó V 2006 *Phys. Rev.* E **73** 021304
[35] Garzó V 2007 *J. Phys. A: Math. Theor.* **40** 10729
[36] Garzó V and Dufty J W 2002 *Phys. Fluids* **14** 1476
 Garzó V, Montanero J M and Dufty J W 2006 *Phys. Fluids* **18** 083305
 Garzó V and Montanero J M 2007 *J. Stat. Phys.* **129** 27
[37] Garzó V 2002 *Phys. Rev.* E **66** 0210308
[38] Garzó V 2007 *J. Stat. Mech.* P02012
[39] Campbell C S 1997 *J. Fluid Mech.* **348** 85